

A negative permeability material at red light

Hsiao-Kuan Yuan, Uday K. Chettiar, Wenshan Cai, Alexander V. Kildishev,
Vladimir P. Drachev, Alexandra Boltasseva, and Vladimir M. Shalaev

Birck Nanotechnology Center, Purdue University, West Lafayette, IN 47907, USA
kildishev@purdue.edu

Abstract: Experimental demonstration of a negative permeability due to near-field coupling of periodic thin silver strips is presented. Two samples with different strip thicknesses are fabricated; optical measurements of the samples confirm our initial design projections by showing the real part of permeability to be about -1 for the sample with thinner strips and -0.8 for the sample with thicker strips at wavelengths of 770 nm and 720 nm.

OCIS codes: (160.4670) Optical materials, metamaterials, negative refraction, left-handed materials; (260.5740) Physical Optics, resonance; (310.6860) Thin films, optical properties.

References and links

1. D. R. Smith, S. Schultz, P. Markoš, and C. M. Soukoulis, "Determination of effective permittivity and permeability of metamaterials from reflection and transmission coefficients," *Phys. Rev. B* **65**, 195104 (2002).
2. A. V. Kildishev, W. Cai, U. K. Chettiar, H.-K. Yuan, A. K. Sarychev, V. P. Drachev, and V. M. Shalaev, "Negative refractive index in optics of metal-dielectric composites," *J. Opt. Soc. Am. B* **23**, 423-433 (2006).
3. U. K. Chettiar, A. V. Kildishev, T. A. Klar, and V. M. Shalaev, "Negative index metamaterial combining magnetic resonators with metal films," *Opt. Express* **14**, 7872-7877 (2006).
4. S. Zhang, W. Fan, K. J. Malloy, S. R. J. Brueck, N. C. Panoiu, and R. M. Osgood, "Demonstration of metal-dielectric negative-index metamaterials with improved performance at optical frequencies," *J. Opt. Soc. Am. B* **23**, 434-438 (2006).
5. J. Zhou, L. Zhang, G. Tuttle, T. Koschny, and C. M. Soukoulis, "Negative index materials using simple short wire pairs," *Phys. Rev. B* **73**, 041101(R) (2006).
6. T. J. Yen, W. J. Padilla, N. Fang, D. C. Vier, D. R. Smith, J. B. Pendry, D. N. Basov, and X. Zhang, "Terahertz magnetic response from artificial materials," *Science* **303**, 1494-1496 (2004).
7. S. Linden, C. Enkrich, M. Wegener, J. Zhou, T. Koschny, and C. M. Soukoulis, "Magnetic response of metamaterials at 100 Terahertz," *Science* **306**, 1351-1353 (2004).
8. A. N. Grigorenko, A. K. Geim, H. F. Gleeson, Y. Zhang, A. A. Firsov, I. Y. Khrushchev, and J. Petrovic, "Nanofabricated media with negative permeability at visible frequencies," *Nature* **438**, 335-338 (2005).
9. A. V. Kildishev, V. P. Drachev, U. K. Chettiar, D. Werner, D.-H. Kwon, and V. M. Shalaev, "Comment on 'Negative Refractive Index in Artificial Metamaterials [A. N. Grigorenko, Opt. Lett., 31, 2483 (2006)],'" submitted to *Optics Letters*.
10. A. V. Kildishev and U. K. Chettiar, "Cascading Optical Negative Index Metamaterials," submitted to the *Journal of Applied Computational Electromagnetics Society*.
11. P. B. Johnson and R. W. Christy, "Optical constants of the noble metals," *Phys. Rev. B* **6**, 4370-4379 (1972).

1. Introduction

A thin film of a nanostructured metamaterial with physical thickness δ can be initially characterized through its spectra to have an effective refractive index $n = n' + \imath n''$ and an effective impedance $\eta = \eta' + \imath \eta''$. In addition, along with its effective n and η , the layer can be characterized by its effective permittivity $\varepsilon = \varepsilon' + \imath \varepsilon''$ and permeability $\mu = \mu' + \imath \mu''$, obtained as $\varepsilon = n/\eta$, and $\mu = n\eta$. The values of n and η (or ε and μ) of the equivalent homogenized layer of thickness δ are chosen to reproduce the complex

values of far-field reflectance and transmittance due to a given film. Using this technique [1,2], the complex values of the transmitted and reflected fields are obtained either from optical experiments or simulations; thus with this method, the effective parameters are always obtained indirectly.

Optical negative index materials (NIMs), also known as left-handed materials, are artificially engineered metal-dielectric composites that exhibit $n' < 0$ within a limited range of wavelengths. In addition, a magnetic resonant behavior should be observed in NIMs at this range. The magnetic resonance in any optical NIM is always required to make the real part of the effective refractive index negative, either through the strong (sufficient) condition $\mu' < 0$ and $\epsilon' < 0$, or through a more general necessary condition $\epsilon'\mu'' + \mu'\epsilon'' < 0$, which is valid for a passive medium. The general condition strictly implies that there is no negative refraction effect in a passive metamaterial with $\mu = 1 + 0i$. Nonetheless, the effect is also achievable for $\mu' > 0$ provided that only $\epsilon' < 0$ in $\epsilon'\mu'' + \mu'\epsilon''$, and $|\epsilon'\mu'| > |\mu'\epsilon'|$. In the latter case, substantial ‘magnetic’ losses are necessary along with a dominant metal content in the structure. We note that a ratio of n'/n'' is often taken as a figure of merit (FOM) for NIM performance, since low-loss NIMs are desirable. The FOM can be rewritten as $|n'/n''| = |\epsilon'|\mu| + \mu'|\epsilon|/|\epsilon''|\mu| + \mu''|\epsilon|$, indicating that a ‘double-negative’ NIM ($\mu' < 0$, $\epsilon' < 0$) will have a much better figure of merit than a NIM layer with $\mu' > 0$. Therefore, metal-dielectric composites with a negative effective permeability are essential for further development of low-loss optical NIMs and their applications.

Our recent computational results [3] have demonstrated that pairs of thin silver strips separated by a dielectric spacer could offer an easy way of achieving negative magnetism by coupling near-field modes. It has also been shown that the magnetic resonance of a periodic array of coupled silver strips with sub-wavelength periodicity is always accompanied by an electric anti-resonance that is fundamentally different from that obtained for the case of an isolated strip pair of the same structural dimensions and materials. Recent studies [3-5] show that the destructive effect of the electric anti-resonance, which makes ϵ' (as well as n') positive, can be straightforwardly compensated by adding background metallic elements (non-resonant strips, homogeneous or inhomogeneous films), and that it is mostly the negative effective permeability that holds the key for advancing the design of low-loss NIMs in optics. Previous important results with different periodic metal-dielectric composites have already been obtained in the terahertz and subsequently in the infrared ranges [5-7]. (Herein, we are not considering a recent report on negative magnetism in the green light range shown in [8]; in our opinion the report is inconclusive, and its ambiguities have been indicated and discussed separately in [9].)

This paper deals with the experimental observation of a negative permeability in the visible range due to near-field coupling of periodic thin silver strips. For our study, two samples (denoted Sample A and B) with slightly different geometries have been fabricated. A negative effective permeability has been retrieved using numerical simulations, and the results are in good agreement with the transmission and reflection spectra obtained from optical measurements of each sample. The value of μ' is about -1 in Sample A and about -0.8 in Sample B at the wavelengths of 770 nm and 720 nm, respectively. In addition to the predicted negative permeability and electric anti-resonances, abnormal anisotropic losses near the resonances are also observed experimentally. Thus, we demonstrate a negative magnetic response from a periodic optical material at visible (red) light and, even more importantly, we discuss new challenges due to significant changes in the optical properties of thin silver strips observed at the resonances.

Figure 1(a) shows an initial ideal elementary cell that we have used to optimize a negative permeability sub-wavelength grating. It consists of a pair of thin silver strips (with thickness t and width w). The strips are separated by an alumina spacer with thickness d , width w , and a refractive index of $n = 1.62 + 0i$. The sub-wavelength lattice constant of the grating is p . The structure has been optimized using custom code based on the spatial harmonic analysis (SHA) approach [10] with additional fabrication constraints pertinent to electron

beam lithography. In the optimal structure the periodicity p was chosen to be 300 nm with $t = 35$ nm, $d = 40$ nm, and $w = 140$ nm, and isotropic bulk optical properties of silver have been taken from [11]. In the resonant (TM) polarization the magnetic field is aligned with the largest dimension – the infinite length of the strips. Only one component of the magnetic field should ideally be present in this case. In the non-resonant (TE) polarization the single component of the electric field is aligned with the strip length, giving no resonant effects. In such an ideal sub-wavelength grating of Fig. 1(a), a relatively wide negative magnetic response exists in the TM regime and extends from a wavelength of 720 nm to 825 nm, as shown in Fig. 1(c). A sharp electric resonance behavior is also demonstrated for the structure in TM mode around 500 nm. The electric resonance introduces a magnetic anti-resonance response within their common wavelength range. A reversed effect is observed at the magnetic resonance, where the electric anti-resonance is now present. The presence of anti-resonance makes it difficult to overlap the magnetic and electric resonances, since as the electric and magnetic resonances get closer to each other the anti-resonances increase in strength, resulting in damping of the resonances [3].

Fig. 1(b) shows a cross-section of the structure adjusted relative to the ideal structure of Fig. 1(a) in order to reflect fabrication realities. Unavoidable imperfections of the fabrication procedure result in a trapezoidal shape of the stacked strips. Therefore, in contrast to the ideal structure, in the actual cross-section the top width w_t is smaller than the bottom width w_b . In addition, two thin 10-nm layers of alumina are added, one between the lower silver strip and the substrate and the second on top of the structure. Both additional alumina layers appear to be necessary for the stable fabrication of samples. Electron beam lithography techniques have been used to fabricate the samples. First, the geometry of the periodic thin silver strips was defined on a glass substrate initially coated with a 15-nm film of indium-tin-oxide (ITO) by use of an electron beam writer. Then, electron beam evaporation was applied to produce a stack of lamellar films. Finally, a lift-off process was performed to obtain the desired silver strips. The projected serial structure of the films from the ITO-coated glass was: Sample A, 10-nm alumina, 30-nm silver, 40-nm alumina, 30-nm silver, 10-nm alumina; Sample B, 10-nm alumina, 35-nm silver, 40-nm alumina, 35-nm silver, 10-nm alumina. As an example of the fabricated structure, a FE SEM image of Sample A is shown in Fig. 2(a).

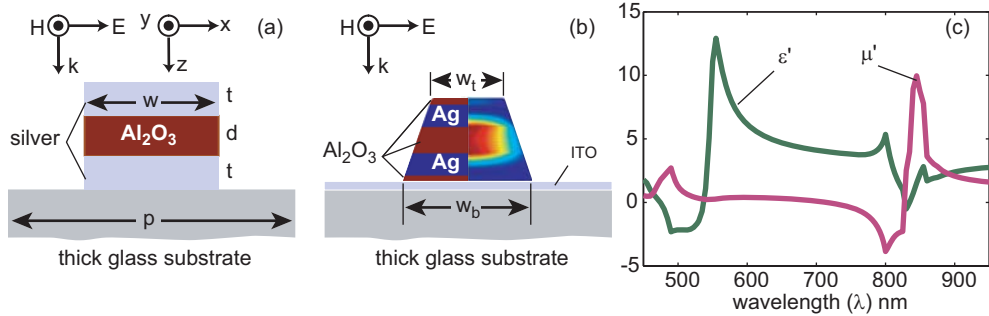


Fig. 1. (a) Ideal unit cell for the array of coupled silver nano-strips of width w are separated by a strip of alumina with the same width, here t is the thickness of both strips, and d is the thickness of the alumina spacer. The strips are infinite in y direction and periodic in x direction with period p . (b) The actual cross-section of samples obtained after fabrication (left half). Right half shows the map of magnetic field enhanced at the magnetic resonance. (c) The real part of permeability and permittivity shown for the cell with $w = 140$ nm, $t = 35$ nm, $d = 40$ nm, and $p = 300$ nm. The optical constants of bulk silver [11] are taken for the strips. The refractive index of the glass substrate is 1.52.

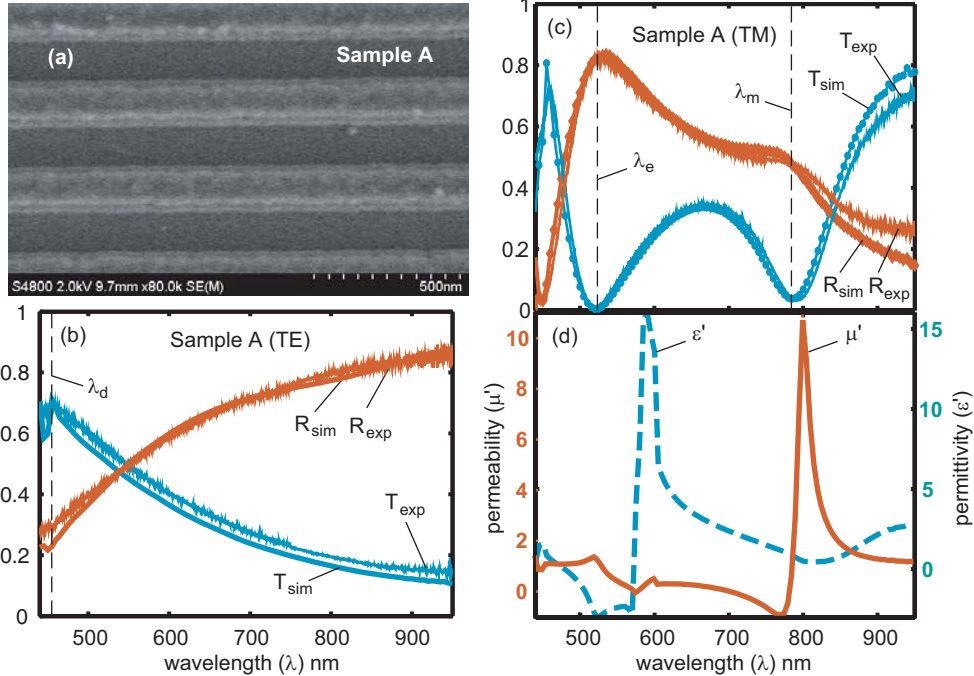


Fig. 2. (a) FE SEM picture of the periodic array of coupled silver strips (Sample A). (b) Transmission and reflection spectra of Sample A measured at normal incidence with TE polarization, here λ_d is the diffraction threshold. The experimental spectra are compared to the results of numerical modeling. The optical constants of silver strips are taken from the experimental data for bulk silver [11] (c) Transmission and reflection spectra of Sample A at normal incidence with TM polarization compared to spectra obtained from simulations. In this case, ϵ'' of the silver strips was adjusted to match excessive losses. (d) The real part of the effective permeability (μ') and effective permittivity (ϵ').

To test the fabricated samples, we measured the transmission and reflection spectra of the samples with an ultra-stable tungsten lamp (B&W TEK BPS100). The spectral range of the lamp covers the entire visible and near-infrared optical band. A Glan Taylor prism was placed at the output of the broadband lamp to select the light with desired linear polarization. The signal transmitted (or reflected) from the sample was introduced into a spectrograph (Acton SpectraPro 300i) and is eventually collected by a liquid nitrogen cooled CCD-array detector. The transmission and reflection spectra were normalized to a bare substrate and a calibrated silver mirror, respectively. In the TE regime the electric field of the incident light was linearly polarized parallel to the length of silver strips, while in TM mode the electric field was rotated 90 degrees relative to TE case. For example, Figs. 2(b) and 2(c) show transmission and reflection spectra obtained from the optical measurements of Sample A for TE and TM polarizations at normal incidence.

In our simulations with a commercial finite element software (more suitable for modeling the exact geometrical details of the structure than the SHA code), an incident plane wave source was placed at the source end of the computational domain, and the transmitted and reflected field amplitudes were monitored at two points located inside the domain several wavelength away from the film under test.

The optical constants of silver used in the ideal model have been initially taken from the experimental data [11] to obtain the optimal structure; as a result, a substantially negative μ' has been obtained, as shown in Fig. 1(c). In the ideal situation, both the experimental and

simulation setup would allow for an adequate match of the reflection and transmission spectra of light in both polarizations. The transmission spectrum with TE polarization is shown in Fig. 2(c). In this case, as expected, both spectra match well over a broad range of measured wavelengths. The measured spectra display a moderate non-resonant wavelength dependence and low, almost constant, absorption; transmission falls off closer to the higher wavelengths. The relaxed wavelength dependence is attributed to non-resonant behavior of the metallic strips diluted with the alumina spacer in a layer that could be adequately described by an effective medium theory. Good matching occurs almost everywhere, provided that the light in the measured and simulated structures has a single propagating mode (no diffraction). Beyond 950 nm, the signal-to-noise ratio worsens, making signal detection difficult at the output.

A useful feature of the optical TE measurements is that the spectral position of the diffraction threshold, shown in Fig. 2(c) as λ_d , is a direct indicator of the true effective periodicity observed in the experiment. Indeed, as long as the refractive index of the substrate, n_s , is known almost exactly, a simple and accurate measurement of the actual period can be obtained from $p = \lambda_d/n_s$.

Similar to the TE mode, the TM polarization gives useful data for measuring the actual geometry of the samples obtained after fabrication. Specifically, the spectral position of the electric and magnetic resonances λ_e and λ_m shown in Fig. 2(c) are both very sensitive to the thickness and width of the metallic strips. Good agreement with the experimental spectra of Figs. 2(c) and 2(b) has been achieved by varying these parameters within realistic fabrication tolerances. Thus, the silver strips used in the simulation of Sample A were 4 nm thinner and 8 nm wider than initial estimates from FE SEM images. Additional examinations of FE SEM images taken in a number of areas over the sample are consistent with this result. As expected, spectroscopic measurements appeared to be more accurate for the dimensions that are critical in the resonant regimes, giving a better result than estimates based on FE SEM images. In addition, clear-cut optical measurements of transmission and reflection spectra with both polarizations incorporate and level out imperfections inevitable in the fabrication process. The dimensions of the samples taken in the simulations are: Sample A, $t = 26$ nm, $d = 48$ nm, $w_t = 94$ nm, and $w_b = 174$ nm; Sample B, $t = 35$ nm, $d = 40$ nm, $w_t = 90$ nm, and $w_b = 160$ nm.

In contrast to TE case, where the optical constants of the bulk silver are used to describe the optical behavior of silver strips, the TM polarization reveals substantial discrepancies in the optical properties of nano-structured silver strips vs. the data shown for bulk silver in [11]. Specifically, the experimental loss is more than that obtained through simulations. This enhanced loss is due to the roughness and other imperfection in the fabricated structure. We model these imperfections through an adjustment factor (α), such that the permittivity of silver is given by, $\epsilon = \epsilon' + i\alpha\epsilon''$. This deviation appears to be significant at the electric and magnetic resonance. Since at the resonances the spatial spectral content of the near-field is radically increasing, we conclude that the near-field modes interact with the inhomogeneities of the silver, resulting in additional losses. The dominant symmetric modes of the electric resonance are less sensitive to the non-idealities of the strips, since relatively smaller adjustments of ϵ'' in silver are necessary around the electric resonance. At the same time, the steeper gradients of the asymmetric modes dominant at the magnetic resonance are much more sensitive to structural defects, dislocations and surface roughness of the strips and a substantial adjustment of losses is required.

Computed results of the transmission and reflection spectra with an adjusted dispersion relation for the permittivity of bulk silver along the non-transverse directions are shown in Figs. 2(c) and 3(c), along with the spectra of adjustment factor α shown in Fig. 3(b). In both samples the adjustment is high at the electric resonance. The adjustment becomes almost one between the two resonances, and eventually reaches its upper level of about six for Sample A and almost seven for Sample B. The additional losses in the resonant regimes of the strips are very large. Unfortunately, these losses diminish the negative magnetic response over the entire range of the magnetic resonance.

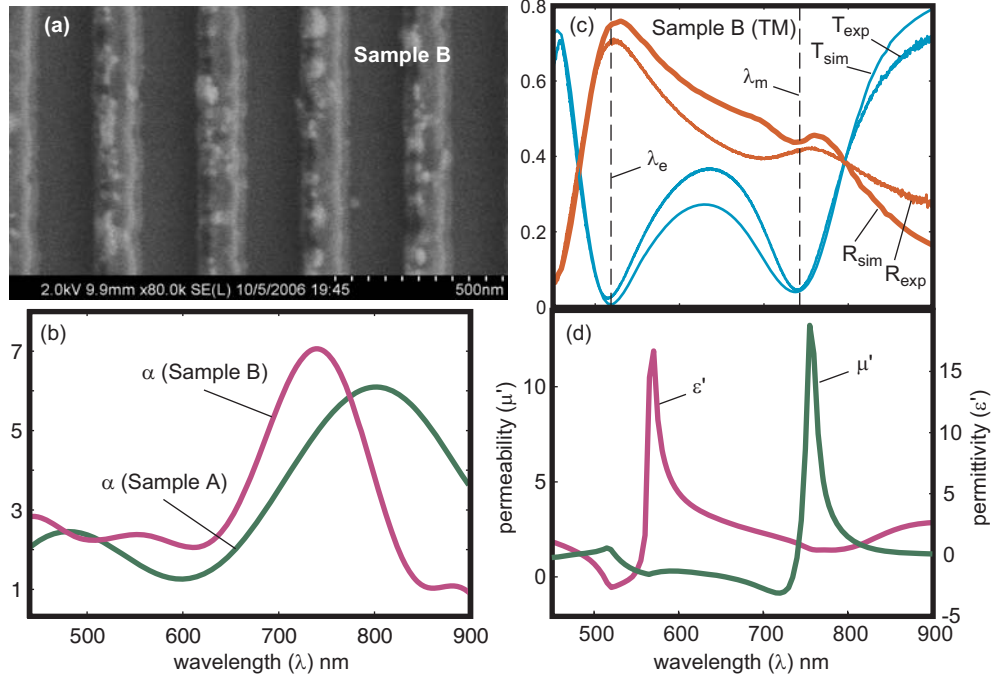


Fig. 3. (a) FE SEM picture of Sample B. (b) Comparison of the loss-adjustment factor α obtained for Samples A and B. Sample B demonstrates more excessive loss in comparison to bulk metal [11] and Sample A. (c) Transmission and reflection spectra of Sample A at normal incidence with TM polarization compared to spectra obtained from simulations. In this case, ϵ'' of the silver strips was adjusted to match excessive losses. (d) The real part of the effective permeability (μ') and effective permittivity (ϵ').

The ideal spectra of μ' computed without any adjustment to the permittivity of bulk silver and the values of μ' calculated with the adjustment factor of Fig. 3(b) have been also compared. Relative to the ideal metal, negative magnetism is reduced by a factor of 7.8 in Sample A and by a factor of 8.8 in Sample B. By measuring and comparing the transmission and reflection of other samples with different fabrication conditions, the average loss adjustment factor of the anisotropic permittivity of silver is estimated to range from six to nine over the entire magnetic resonance. Although the actual range of the adjustment factor α depends greatly both on the initial design of the magnetically resonant structure and its fabrication conditions, these estimates provide approximate margins for the adjusted values of losses in resonant nano-structured silver structures in the visible light range.

In summary, we designed, fabricated and measured two samples with negative permeability of -1 and -0.8 at 770 nm and 720 nm, respectively. Detailed numerical models of the samples have been used to validate the measurements, where an adjusted wavelength-dependent ϵ'' is used in silver at the resonances. The results of the numerical modeling are compared with the experimental data. The good agreement between experiment and theory achieved for two different polarizations in a wide range of wavelength is an excellent confirmation of the validity of the model, hence confirming the existence of negative permeability at red light. We also discuss the difficulties in automated optimization of NIMs due to substantial deviations from the properties of bulk metal observed experimentally in the resonant plasmonic elements of our nano-structured samples. These deviations would require constant feedback from fabrication and measurements for obtaining double-negative NIMs in visible range.